Pulse-duration memory effect in $NbSe_3$ and comparison with numerical simulations of phase organization

T. C. Jones, Xinlei Wu, C. R. Simpson, Jr., J. A. Clayhold, and J. P. McCarten
Department of Physics and Astronomy, Clemson University, Clemson, South Carolina 29634-1911
(Received 3 May 1999; revised manuscript received 21 December 1999)

The oscillatory response of the 59 K charge density wave (CDW) in $NbSe_3$ to a sequence of current pulses was investigated as a function of pulse height and pulse width. Of the 16 samples investigated, seven clearly exhibited the learned behavior commonly referred to as the pulse-duration memory effect (PDME). These seven samples, after training, learned the length of the pulse, and always finished the pulse at a minimum in the voltage oscillation (maximum CDW velocity). Contrary to previous reports, we observe the PDME for pulse heights much greater than threshold. We find that as the number of metastable states accessible to the CDW during the low portion of the drive pulse is decreased, the PDME degrades. We summarize the qualitative differences between the theory of phase organization and the observed experimental data. To facilitate this comparison we have performed numerical simulations of the Fukayama-Lee-Rice (FLR) model in both the weak and strong pinning limits in an attempt to reproduce the learned response. We find no evidence for phase organization (no learning) in the weak pinning limit; also the wave forms generated in the strong pinning limit differ qualitatively from the experimental data. This comparative study suggests that the theoretical description of the PDME requires further investigation, and the importance of amplitude collapse and boundary conditions demand future examination.

I. INTRODUCTION

Above a threshold current (voltage) an incommensurate charge density wave will depin from the impurities and other crystalline defects, and effectively *slide* through the crystal creating a new conduction channel.[1] Due to the large number of available metastable pinned states below threshold, CDWs exhibit a rich variety of memory effects.[2–6] Of these the pulse duration memory effect is the most remarkable.[7–9] Upon application of a series of identical unipolar current pulses, the voltage response appears to defy *causality* by learning when the current pulse is going to end. The learning is due to the special metastable state that the CDW relaxes into between pulses. This metastable state effectively encodes the length of the previous pulse. Experimentally if the same current pulse is applied after training, then the oscillating voltage response always finishes the pulse at an oscillation minimum. A multiple pulse-duration memory effect has also been observed.[10]

Like a superconductor, the superlattice of the CDW is described by a complex order parameter $\Delta e^{i\phi}$. Here Δ is proportional to the amplitude of the superlattice distortion, and ϕ the phase. Many investigators believe that the essential physics of the PDME can be described with only the phase degrees of freedom.[11,12] Numerical investigations of phase-only models, such as the classical Fukayama-Lee-Rice (FLR) model, and the similar Frenkel-Kontorova model, have provided insight into the PDME.[11,12] Computer simulations find that for repetitive driving pulses the phase degrees of freedom relax into a special metastable state such that if the same driving pulse is again applied, all the degrees of freedom finish the pulse near a point of maximum potential energy. Termed phase organization, this alternative pattern formation behavior has many significant implications. For instance, in a steady state the metastable configuration into which the CDW relaxes between pulses is the highest-energy (maximally strained) metastable configuration.[11] The fact that the dynamics selects configurations of minimal stability has significant implications for the statistical mechanics of the system. The usual approach of minimizing the global free energy would incorrectly weight the most stable (minimally strained) configurations as most probable.

The theory of self-organized critical behavior follows from the concept of phase organization.[13] Today researchers are investigating the use of self-organized dynamical systems for a variety of numerical computations.[14] Given all this theoretical work, very little attention has been given to whether the theory of phase organization correctly describes CDW dynamics. Okajima and Ido,[8] and also Ito[15] have suggested that amplitude collapse cannot be neglected, and that the PDME is due to the organization of slip events. We will adress the issue of amplitude collapse in detail in Sec. V.

In this paper we report both experimental studies of the PDME in high-quality $NbSe_3$ single crystals, and numerical studies of the phase only FLR model in both the weak and strong pinning limits. In Secs. II and III we present our experimental methods and the data. Section IV describes our numerical simulations. Section V compares experiment and theory, and discusses a number of inconsistencies between the two. We conclude in Sec. VI.

II. EXPERIMENT

For this study we used high-quality single crystals of undoped $NbSe_3$ from a growth with residual resistance ratios $[\rho(300\ \mathrm{K})/\rho(4.2\ \mathrm{K})]$ over 300. These crystals grow as long needles with typical dimensions $1\mathrm{cm}\times 10\ \mu\mathrm{m}\times 1\ \mu\mathrm{m}$. Previous x-ray studies[16] and impurity-doping studies[17] find a CDW superlattice phase-phase correlation length in excess

of 100 μm in the direction of the needle axis for crystals of this quality. A phase-coherent domain contains over 10^7 impurities,[17] therefore these crystals are well into the weak impurity pinning limit.

Samples were mounted with silver paint in the standard four-wire configuration, and cooled using a closed-cycle helium refrigerator. Helium-exchange gas ($\frac{1}{2}$ atmosphere) was added to the sample to minimize ohmic heating. Temperature was controlled to ± 1 mK. After the contact resistance was determined to be less than 5% of the total sample resistance, pulse measurements were performed using only the inner leads (two-probe method). Current pulses were created using a Stanford DS345 function generator and a large resistor (typically 100 kΩ) in series with the sample. Voltage wave forms from the sample were captured using a Tektronix TDS744 digitizing oscilloscope, set to a bandwidth of 20 MHz. Since the crystal cannot be properly terminated, lead lengths were held to less than 0.1 m to minimize reflections.

For this study we only investigated the 59-K CDW transition, and focussed primarily on temperatures for which the threshold voltage for CDW depinning (V_T) is nearly a minimum. Previous studies find that this is the temperature where ac-dc mode locking and pulsed mode locking are most likely complete.[18] This is also the temperature range where the amplitude of the voltage oscillation, hereafter referred to as the narrow band noise (NBN), is largest in comparison to V_T.

Contrary to ac-dc mode locking, pulsed mode locking is not mode locking in a strict meaning. For the ac-dc case the mode locking is a dynamical phenomena, which occurs when the frequency of the NBN under a dc-bias locks onto the harmonics or subharmonics of the external ac-bias frequency. Pulsed mode locking is nearly independent of the length of time between pulses (see Sec. III). This means the CDW fully relaxes between pulses.

Experimentally characterizing the pulsed mode locking is difficult, and was not the focus of this study. If the CDW is mode locked onto a p/q cycle, then the superlattice advances p CDW wavelengths every q cycles. However voltage wave forms alone cannot deduce the value of q.[18] For example, what appears to be a 3/1 cycle could be a 6/2 or a 9/3 cycle. We will only note that $q=1$ locking appeared to dominate most regions of drive parameter space because the voltage response from pulse to pulse was nearly identical for a given repetitive drive sequence. Data shown in Figs. 1, 2, and 3 are from our most coherent sample. Wave forms shown are averaged 50 times to reduce noise, but the same functional form was clearly evident from single-shot measurements.

III. DATA

We examined 16 different samples. Application of a dc current of a few times threshold typically produced a NBN signal of 20 μV_{px-p}. As summarized in Table I, significant amplification of the NBN occurred in 11 of the samples for a repetitive unipolar pulse sequence. For these samples the voltage response from pulse to pulse was nearly identical, suggesting most of the crystal was mode locked on a $q=1$ cycle. The crystals, for which there was little to no amplification of the NBN, typically had larger cross sectional areas, implying CDW velocity coherence is more difficult to maintain in larger samples. Of the 11 crystals that showed NBN amplification, only seven exhibited the PDME. The voltage oscillation for all seven of these crystals finished the current pulse at a minimum in the oscillation, independent of pulse width (t_{high}), for 1.0 μs$<t_{high}<$10 μs. For $t_{high}<1.0$ μs the PDME begins to slowly degrade. For $t_{high}>10$ μs the amplitude of the voltage oscillation decays in magnitude, making it difficult to resolve the data. However for the few samples for which we could resolve the data, the PDME was evident at these longer pulse widths. We have no explanation as to why the PDME was not observable in four samples, i.e., the voltage oscillation could finish the pulse increasing or decreasing depending on drive parameters. This may be due to contact effects and requires further investigation.

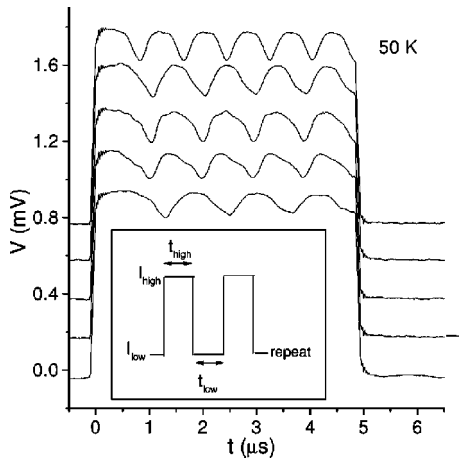

FIG. 1. Wave forms of the voltage response for Sample A to repetitive unipolar current pulses of five different $I_{high}I_{high}$ for each wave form is 9.51 μA, 9.70 μA, 9.90 μA, 10.10 μA, and 10.30 μA from bottom to top. $I_{low}=0$ and $t_{high}=t_{low}$. At this temperature $V_T=0.69$ mV and $I_T=6.93$ μA. Wave forms are averaged 50 times to reduce noise. Curves are offset 0.2 mV for clarity. Inset is a schematic of the current drive. For a dc current drive of 32 μA the amplitude of the NBN voltage oscillation is only 24 μV_{p-p}. During the low portion of the pulse the voltage is not quite zero due to a small thermally-induced offset.

Figures 1–4 illustrate one of the main results of this paper: after training the voltage always finishes the pulse at a

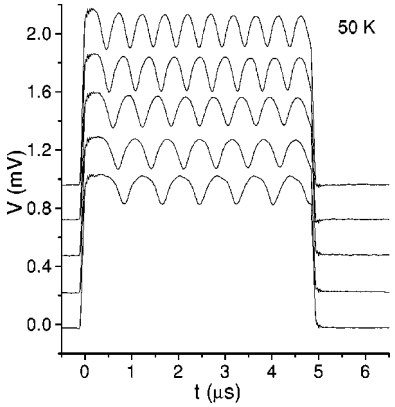

FIG. 2. Continuation of Fig. 1. The voltage oscillation always finishes the pulse at an oscillation minimum (maximum in CDW velocity). I_{high} for each wave form is 10.50 μA, 10.89 μA, 11.49 μA, 11.88 μA, and 12.67 μA from bottom to top. Curves are offset 0.25 mV for clarity.

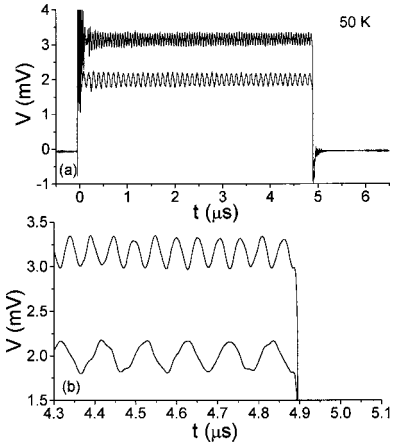

FIG. 3. (a) Continuation of Figs. 1 and 2. I_{high} is 32.08 μA (bottom) and 56.63 μA (top). The PDME is still evident for drive amplitudes approaching $10I_T$. Larger drive amplitudes were not measurable due to alias. The initial large amplitude oscillation between 0 and 0.2 μs is LRC ringing due to the leads. (b) Waveforms expanded near the end of the pulse.

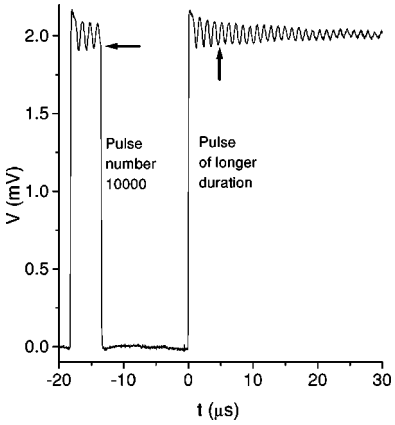

FIG. 4. Wave form of the voltage response for Sample B to a repetitive unipolar current pulse sequence, showing the response for pulse number 10 000, followed by a pulse of much longer duration (75 μs). Data illustrates that after training the CDW clearly finishes the pulse at a point of maximum velocity (minimum voltage). Left-most arrow indicates that the CDW finishes the pulse at an oscillation minimum; right-most arrow indicates the duration of the training pulses. $I_{high}=25.0$ μA, $I_{low}=0$, $t_{high}=5$ μs, and $t_{low}=13.5$ μs. $T=49$ K. At this temperature, $V_T=1.5$ mV, and $I_T=17$ μA. Wave forms are averaged 20 times to reduce noise.

minimum in the voltage oscillation (maximum CDW velocity). Data shown in Figs. 1–3 is from the most coherent sample of this study, Sample A. The PDME was clearly evident even for the largest drive amplitude we could measure ($I_{high}\approx 10I_T$). This differs from previous studies where the PDME was only observed for drive amplitudes less than twice threshold.[8] We did observe degradation in the PDME for $I_{high}>3I_T$ for Samples D–G, however Sample A indicates this degradation is due to extrinsic effects such as spatial inhomogeneities in the pinning force.

Sample A also illustrates the remarkable enhancement in NBN signal in the pulsed mode-locked state. For a dc current drive of 32 μA the amplitude of the NBN is only 20 μV_{p-p}. In Fig. 3, the NBN amplitude for the repetitive 32-μA pulse sequence is a remarkable 370 μV_{p-p}; this peak-peak amplitude is greater than $V_T/2$. This data strongly suggests that in the mode-locked state all degrees of freedom move in phase, or at least nearly in phase.

Theoretically the number of metastable states available to

TABLE I. Summary of the 16 samples that were part of this study. We investigated unipolar current pulses with $I_T<I_{high}<3I_T$, 1.0 μs$<t_{high}<10\mu$s, $I_{low}=0$, and $t_{high}=t_{low}$ (see inset Fig. 1) for all samples. If the voltage oscillation during the high portion of the drive sequence was less than 50 μV_{p-p}, we did not attempt to determine if the sample exhibited the PDME. ''Yes'' in the PDME column indicates that for a large region of drive parameter space the voltage oscillation always finished the pulse at an oscillation minimum. Most samples did not exhibit the PDME for $t_{high}<1.0$ μs. Length is the distance between voltage contacts.

Sample	Length (μm)	Width (μm)	Thickness (μm)	Oscillation amplitude >50 μV_{p-p}	PDME
A	390	3±1	1.3±0.4	Yes	Yes
B	820	5±1	1.0±0.2	Yes	Yes
C	1100	10±1	0.25±0.05	Yes	Yes
D	630	2±1	0.5±0.25	Yes	Yes
E	550	4±1	0.3±0.1	Yes	Yes
F	750	4±1	0.6±0.2	Yes	Yes
G	360	3±1	0.6±0.2	Yes	Yes
H	950	6±1	1.2±0.3	Yes	No
I	830	3±1	0.5±0.2	Yes	No
J	350	9±1	0.10±0.02	Yes	No
K	740	14±1	0.9±0.1	Yes	No
L	520	11±1	2.5±0.3	No	N/A
M	650	19±1	0.5±0.05	No	N/A
N	600	13±1	0.6±0.05	No	N/A
O	1200	15±1	0.7±0.1	No	N/A
P	1200	12±1	0.4±0.05	No	N/A

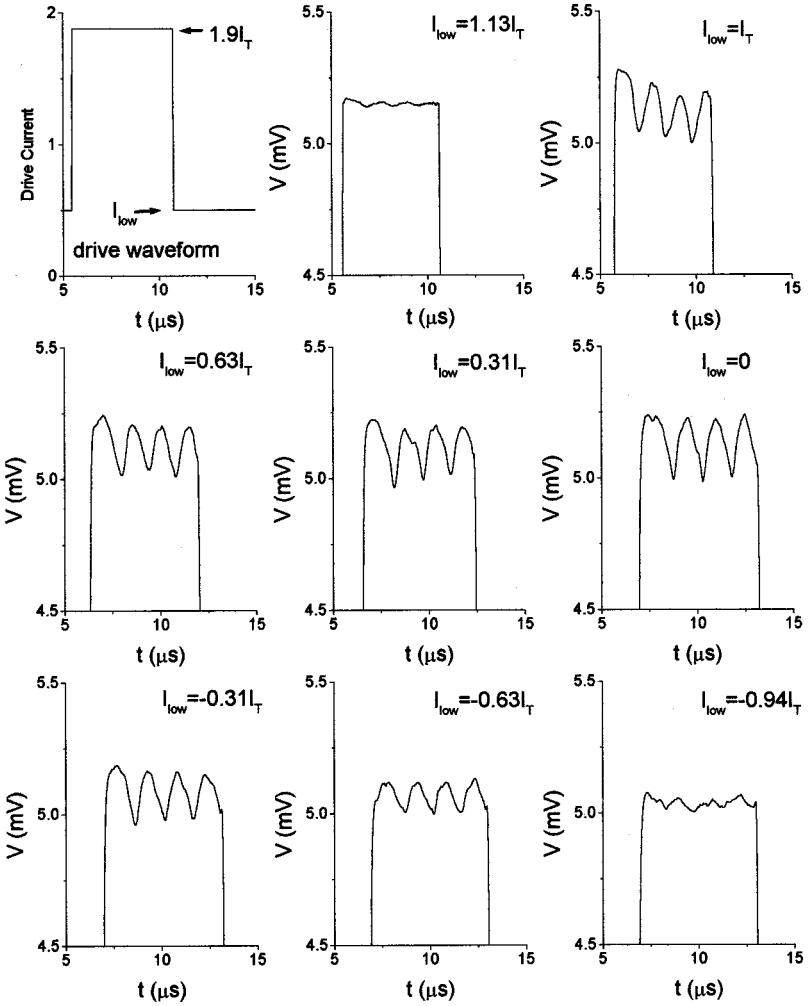

FIG. 5. Wave forms of voltage response for Sample C to repetitive unipolar current pulses. I_{low} is varied, and $I_{high}=1.9I_T$, as illustrated in the upper-left figure. t_{high} is such that the voltage wave form contains four oscillations. As the magnitude of I_{low} approaches I_T, the magnitude of the voltage oscillation decreases, and the PDME is no longer evident (see Fig. 7). Wave forms are averaged 25 times to reduce noise. $t_{low}=15$ μs. $T=45$ K. At this temperature $I_T=8.0$ μA, and $V_T=2.8$ mV. For a dc current drive of 15 μA the amplitude of the voltage oscillation is only 18 μV_{p-p}.

the CDW system decreases as the dc current drive I approaches I_T.[19] For the phase-only model there is only one pinned configuration available to the system at threshold. To investigate how the number of metastable states accessible to the CDW during the low portion of the pulse influences the PDME we have investigated pulse sequences where $I_{low} \neq 0$. This data is summarized in Figs. 5–7.

Figure 5 illustrates that the NBN amplitude decreases significantly if $I_{low}>1.1I_T$ or $-0.7I_T>I_{low}$. For positive I_{low} the dramatic reduction in NBN amplitude occurs at a value slightly greater than the dc threshold. The reason the drop does not occur at I_T is because threshold for the dc case and threshold for the $t_{low}=15$ μs case do not coincide. The decrease in NBN amplitude occurs more rapidly for negative values of I_{low}. This indicates that there is a distribution of CDW velocities associated with repolarization. Figure 6 shows the regimes of $I_{low}-t_{high}$ space in which three, four, and five oscillations were clearly observed in the voltage response wave forms.

The PDME degrades as $|I_{low}|$ increases above zero, but the degradation is gradual. Figure 7 shows voltage wave forms for 5 different t_{high} with $I_{low}=0.94I_T$. For this value of I_{low} there should be very few metastable states accessible to the CDW during the low portion of the pulse. As predicted

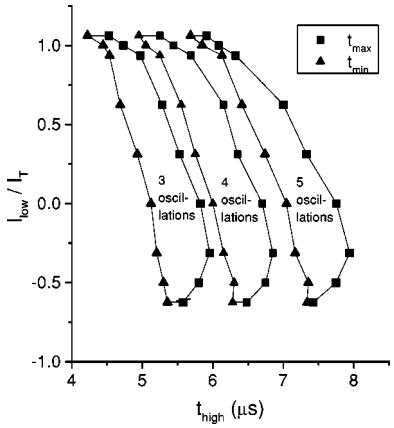

FIG. 6. Regions of $I_{low}-t_{high}$ space in which three, four, and five oscillations were clearly observed in the voltage response wave forms for Sample C. (We assume these correspond to the 3/1, 4/1, and 5/1 mode-locked steps.) Current drive wave form is the same as in Fig. 5; $I_{high}=1.9I_T$, and I_{low} is one parameter of the phase space diagram. The PDME is evident for $-0.4I_T<I_{low}<0.8I_T$; when I_{low} exceeds this range, the voltage wave form does not necessarily finish the pulse at an oscillation minimum (see Fig. 7). For $I_{low}>1.1I_T$ or $-0.6I_T>I_{low}$ the amplitude of voltage oscillation is greatly reduced (see Fig. 5).

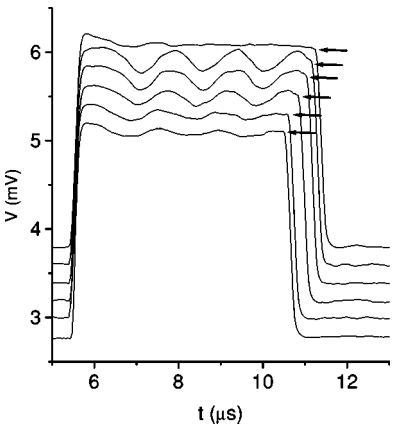

FIG. 7. Wave forms of voltage response of Sample C to repetitive unipolar current pulses for different t_{high}. Current drive wave form is the same as in Fig. 5 with $I_{low}=0.94I_T$. Starting from the bottom curve, each is offset in steps of 0.2 mV for clarity. Arrows indicate there is no PDME because the wave form does not necessarily finish the pulse at an oscillation minimum.

by the theory of phase organization, the data does not exhibit the PDME because the wave forms do not necessarily finish the pulse near the oscillation minimum. Interestingly, if the voltage oscillation finishes the pulse near a minimum, then those wave forms possess a larger NBN amplitude. We have noticed that this is a general feature seen for all samples, independent of drive parameters.

For completeness we also investigated the dependence of t_{low} on the NBN amplitude for Samples B, C, and D. Figure 8 is typical of all three samples; the NBN amplitude is a maximum for t_{low} near 4 μs, and decreases slowly very with increasing t_{low}. Experimentally we find that the PDME degrades rapidly with decreasing t_{low} below 1.0 μs. For 1.0 $\mu s<t_{low}<1.0$ ms the PDME was robust for all three samples. Quantifying the learned behavior with increasing t_{low} beyond 1.0 ms is more difficult. For Sample C the PDME did not degrade substantially with increasing t_{low} up to the longest time we investigated (10 s). For both Samples B and D a noticeable degradation set in with increasing t_{low} above 1.0 ms. This suggests that the destruction of the encoded metastable state by thermal fluctuations is sample dependent.

Finally, the number of pulses necessary to train the CDW for different initial conditions will be the topic of a longer paper, and is briefly elaborated on in Sec. V.

IV. SIMULATIONS

Comparing the experiment with the phenomenological single-coordinate model (SCM) provides some insight into

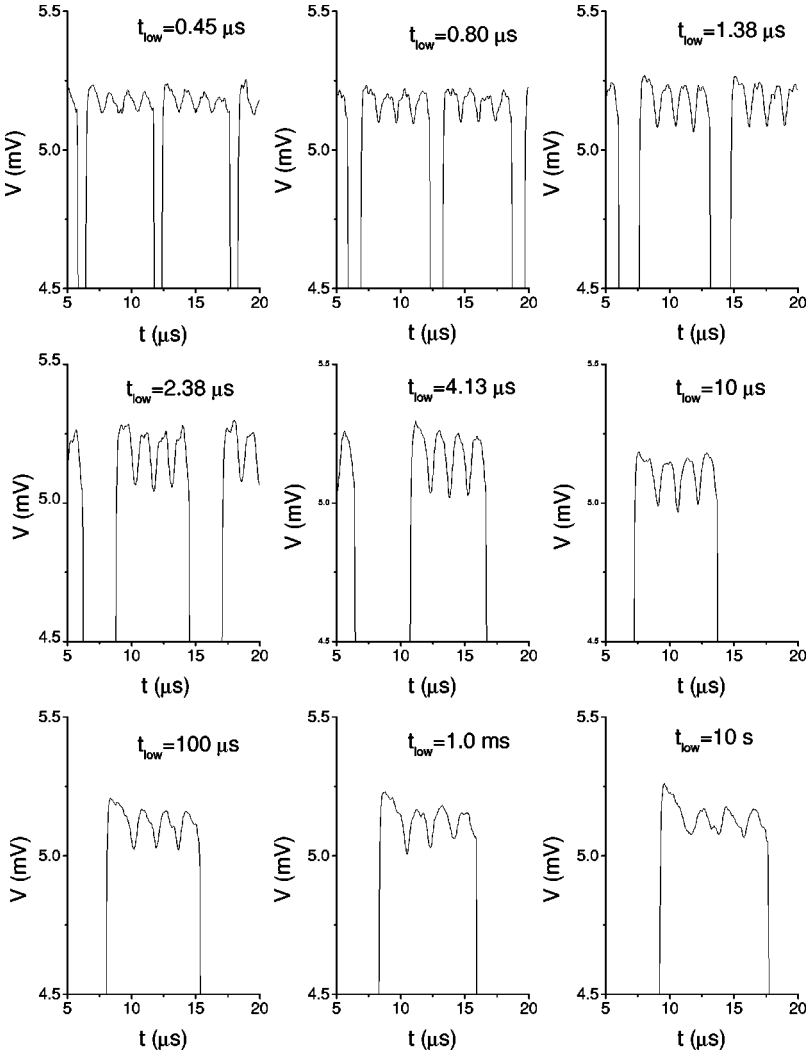

FIG. 8. Wave forms of voltage response of Sample C to repetitive unipolar current pulses for different t_{low}. $I_{high}=1.9I_T$ and $I_{low}=0$. t_{high} was selected such that the voltage wave form produced four oscillations. Oscillation amplitude is a maximum for t_{low} near 4.13 μs. The PDME is only evident for $t_{low}>1.0$ μs (see text).

why the PDME is so remarkable. The SCM is mechanically equivalent to a driven pendulum in the overdamped limit. The phase changes in time according to

$$\gamma \frac{d\phi}{dt} = V - V_T \sin(\phi). \tag{1}$$

Note that γ is a phenomenological damping constant, and $d\phi/dt$ is proportional to the CDW current. The experimental observation that the voltage oscillation finish the pulse at a minimum implies that $\phi_{end} = 3\pi/2 + (\text{integer})2\pi$, where ϕ_{end} is the phase of the CDW at the end of the pulse. However, for a driving pulse of arbitrary height or width, this model cannot reproduce the learned behavior. Assuming the CDW fully relaxes between pulses then $\phi_{initial}$ is equal to an integer multiple of 2π. For an arbitrary current pulse ϕ_{end} can take on any value, and therefore the induced V oscillation for the SCM can finish the pulse at any point, not necessarily at a minimum. This suggests the internal degrees of freedom of the CDW are responsible for the learned behavior.

Several groups have attempted to numerically simulate the PDME using the Fukuyama-Lee-Rice model.[20] One group successfully modeled the learned behavior,[12] one was partially successful,[15] and another was unsuccessful.[21] The impurity pinning limit appears to have been the cause of the discrepancy. To investigate this discrepancy we have simulated the FLR model in both the weak and strong pinning limits.

The validity of the FLR model as a description for CDW systems has been discussed at length elsewhere, along with the procedure for discretizing the equation of motion.[20,22] The discretized equation of motion in one dimension (1D) in the presence of an external electric field E is given by

$$\gamma \frac{d\phi_n}{dt} = E - \varepsilon \sin(\phi_n - \beta_n) - \kappa(\phi_{n+1} + \phi_{n-1} - 2\phi_n). \tag{2}$$

Here, n represents the site index ($n = 1,2,\ldots,N$) and $d\phi_n/dt$ is proportional to the local CDW velocity. The mechanical analogy to a system of pendulums is quite useful. A pendulum with phase ϕ_n is in a viscous medium with damping constant γ, and elastically coupled to neighboring pendulums with coupling constant κ. Each pendulum experiences a torque E. It is affected by a pinning force of strength ε with random phase β_n. The fixed random variable β_n effectively disorders the direction of the gravitational field at each site, which models the random distribution of impurities for the actual CDW.

The dimensionless pinning parameter ε/κ determines the strength of the pinning. If $\varepsilon/\kappa < 1$, then the system is in the weak pinning limit and the static ($E = 0$) phase-phase correlation length is equal to $3.5(\varepsilon/\kappa)^{-2/3}$ assuming an impurity on every lattice site.[22] For the strong pinning limit the static phase-phase correlation length is just one lattice site. For all numerical results reported here $\gamma = 1$, $\kappa = 1$, and the boundary conditions are cyclic.

For numerical investigations it is simpler to examine the spatially averaged current response ($\langle d\phi_n/dt \rangle_n$) to a sequence of repetitive E pulses, instead of the experimental situation of the electric field response to a sequence of current pulses. Comparison between the different types of pulse drives is straightforward. For the current drive experiments, a maximum CDW velocity corresponds to a minimum in the voltage oscillation.

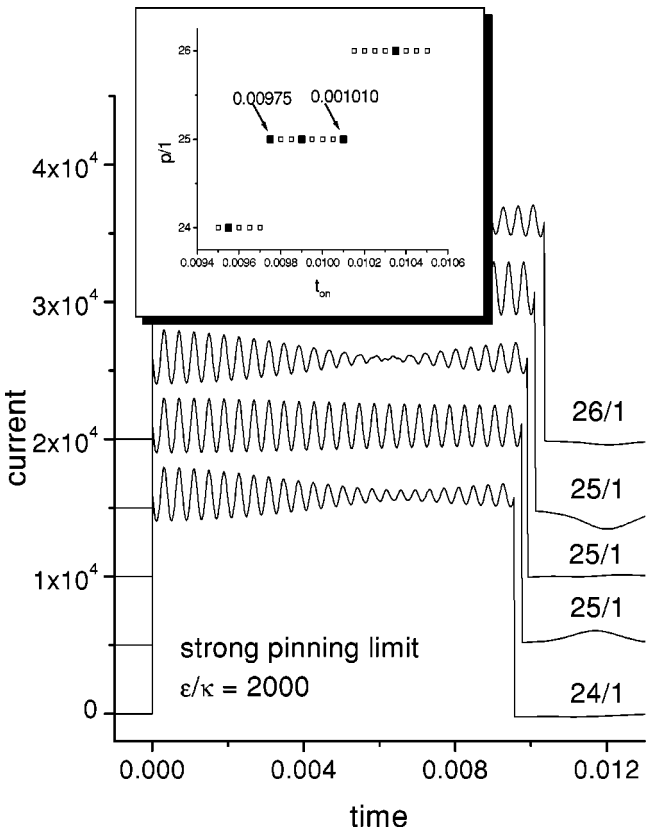

FIG. 9. Simulated CDW current response to a sequence of unipolar electric field pulses for five different pulse lengths. System is moded-locked onto a $q = 1$ cycle. $E_T = 2000 \pm 5$. $E_{high} = 7.5E_T$, $E_{low} = 0$, and $t_{low} = 0.5$. From bottom to top pulse lengths are 0.009 55, 0.009 75, 0.009 95, 0.010 15, and 0.010 35. Phase organization is evident from the data since the current finishes the pulse increasing. The beating of the wave forms is discussed in the text. There are 128 degrees of freedom. Initial conditions are highly strained. Curves are offset for clarity.

Our simulations in the strong pinning limit are consistent with the theory of phase organization.[11] As shown in Fig. 9 the CDW current always finishes the pulse increasing at the midpoint between the maximum and minimum in the amplitude of the current oscillation. This point on the wave form is a signature of phase organization, and implies the phase degrees of freedom finish the pulse at a point of maximum potential pinning energy. We have verified this numerically by checking to see that $\phi_n - \beta_n$ finishes the pulse near a value of $\pi + (\text{integer})2\pi$ for each degree of freedom (see Figs. 10 and 11). For this set of simulations the initial metastable state was highly strained. This metastable state was obtained by setting each phase variable to a random number between -10^6 to 10^6 and letting the system relax. If instead we begin with a metastable state near the ground state ($\phi_n \cong 0$ for all n), then we do not observe phase organization. The lack of phase organization for initial conditions near the ground state has been discussed at length by Ito.[15] Behavior similar to the SCM is recovered for these initial conditions.

The beating exhibited for pulse lengths near the center of

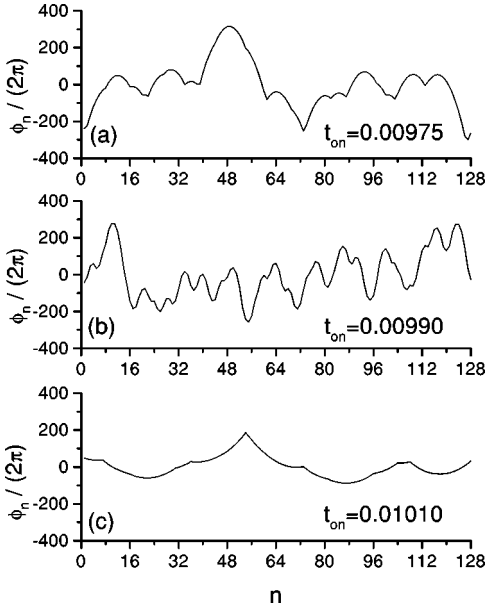

FIG. 10. CDW phase as a function of position at the end of a pulse. Numerical data are for steady state, and correspond to the numerical data of Fig. 9. Near the edges of the 25/1 step (t_{on} = 0.009 75, 0.010 10) the overall strain is reduced in comparison to the center of the 25/1, but there are a few sharp kinks.

the $q=1$ steps in Fig. 9 is simple to understand. According to the theory of phase organization the system selects a special metastable state to relax into for a $q=1$ mode-locked cycle. This metastable state is such that at the end of the next pulse the phase degrees of freedom form fall-forward and

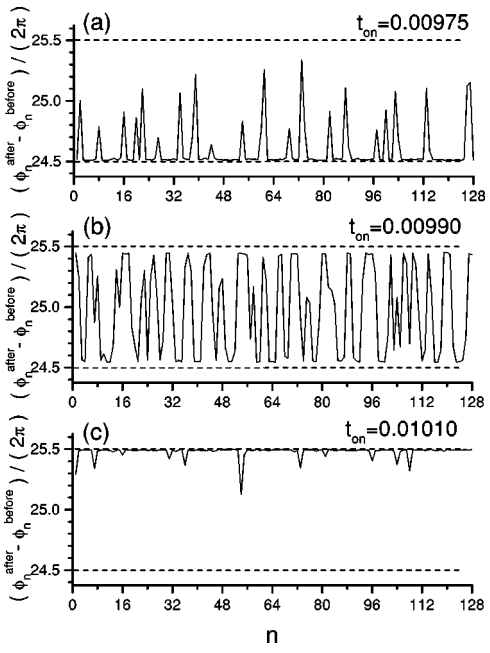

FIG. 11. CDW phase difference from just before the pulse to just after, as a function of position. Numerical data are for steady state, and correspond to the numerical data of Fig. 9. Note that the data is heavily weighted at 24.5π and 25.5π. The 24.5π regions advance 0.5π after the pulse is turned off, and the 25.5π regions retreat 0.5π. These correspond to the the fall-forward and fall-back regions of phase organization.

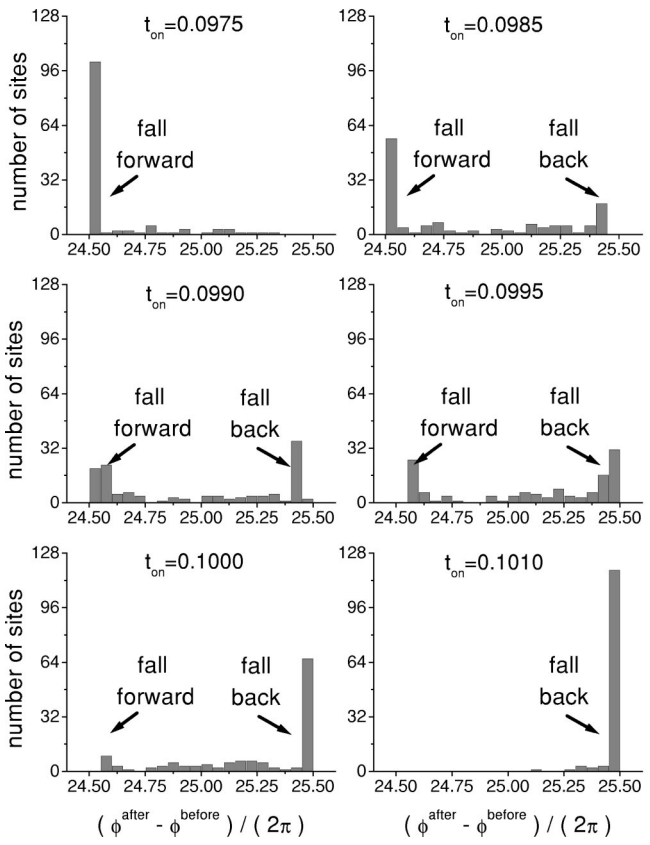

FIG. 12. Histograms of the CDW phase difference from just before the pulse to just after, for six different t_{on} values for the 25/1 step. Numerical data are for steady state, and correspond to the numerical data of Fig. 9. Note that the data is bimodal, and clearly shows the the fall-forward and fall-back regions of phase organization. Near the step edges (t_{on} = 0.0975,0.1010) the phase difference is mostly fall forward or mostly fall back.

fall-back regions.[15] During the pulse the degrees of freedom in a fall-forward region advance $p-1/2+\delta$ ($\delta<<1$) winding numbers and fall forward after the pulse is turned off; those in a fall-back region advance $p+1/2-\delta$ winding numbers and fall back. As illustrated in Fig. 12 for regions of parameter space (pulse height–pulse width) near the center of the $p/1$ step, the phase degrees of freedom are equally divided between fall-forward and fall-back regions. Therefore halfway through the pulse these two sets of degrees of freedom are out of phase, resulting in a node in the wave form. For regions of parameter space (pulse height–pulse width) near the edge of the $p/1$ step, all the phase degrees of freedom form a single fall-back or a single fall-forward domain, and no beating occurs.

Figure 13 shows results for simulations in the weak pinning limit ($\varepsilon/\kappa=1/8$). Since the static phase-phase correlation length is 14, we increased the number of lattice sites to 2048 to ensure we captured the dynamics of the internal degrees of freedom. Evidence of phase organization in the current wave forms is very weak; the CDW current oscillation does finish the pulse increasing, but the position varies from near the oscillation minimum to near the oscillation maximum depending on drive parameters. Evidence for phase organization was even weaker for the other pulse drives we investigated; $E_{on}=12E_T$ or $1.5E_T$, and t_{on}

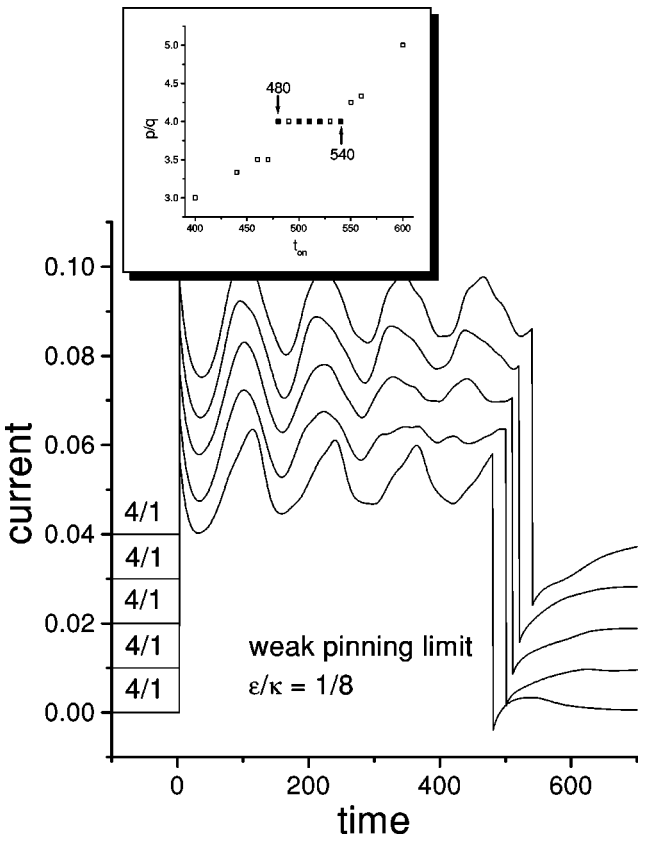

FIG. 13. Simulated CDW current response to a sequence of unipolar electric field pulses for five different pulse lengths. The system is moded locked onto a $q=1$ cycle. $E_T=0.026\pm0.001$. $E_{high}=3E_T$, $E_{low}=0$, and $t_{low}=7000$. From bottom to top pulse lengths are 480, 500, 510, 520, and 540. Wave forms differ greatly compared with the strong pinning limit. There are 2048 degrees of freedom. Initial conditions are highly strained. Curves are offset for clarity.

$=5000$. Like the numerical data shown in Fig. 9, that shown in Fig. 13 is for highly strained initial conditions. The initial metastable state was obtained by setting each phase variable to a random number between -10^5 to 10^5 and letting the system relax. Figures 14–16 illustrate that the degrees of freedom do not separate into fall-forward and fall-back regions, indicating a lack of phase organization in the weak pinning limit.

Finally we note that just as for the strong pinning limit, if instead we begin with a metastable state near the ground state ($\phi_n\cong0$ for all n) the response is similar to the single-coordinate model (see Fig. 17).

Comparison with the extensive numerical calculations by Ito is enlightening.[15] These simulations were in the intermediate pinning limit. He finds that for a wide range of initial conditions, the FLR model selects a metastable state such that in steady state all the phases advance $\cong2\pi n$ during the pulse, where n is an integer. These results are consistent with our weak pinning limit simulations (see Fig. 16), and differ greatly from that of the phase organization, where the phases advance $\cong2\pi n\pm\pi$.

As noted by Ito there is an important discrepancy between his simulations of the FLR model and the experiment. A phase advancement of $2\pi n$ corresponds to the voltage oscillation ending the pulse with a downward slope near the mid-

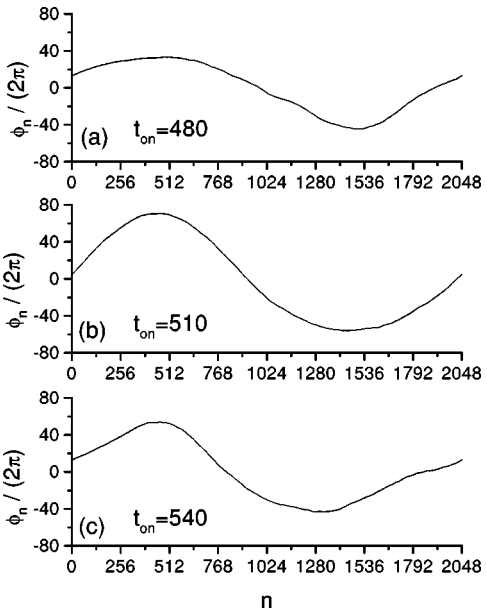

FIG. 14. CDW phase as a function of position at the end of a pulse. Numerical data are for steady state, and correspond to the numerical data of Fig. 13. The global CDW strain is slightly smaller near the edges of the 4/1 step ($t_{on}=480,540$), compared with data near the step center ($t_{on}=510$).

point, in contrast to the experiment, where the voltage oscillation finishes the pulse at a minimum. In Ito's opinion, this discrepancy results from the fact that the relation between the sliding displacement and the phase in the current oscillation between the FLR model and the experiment do not agree. This is a very important point, suggesting that a phase-only model is insufficient to describe the experiment.

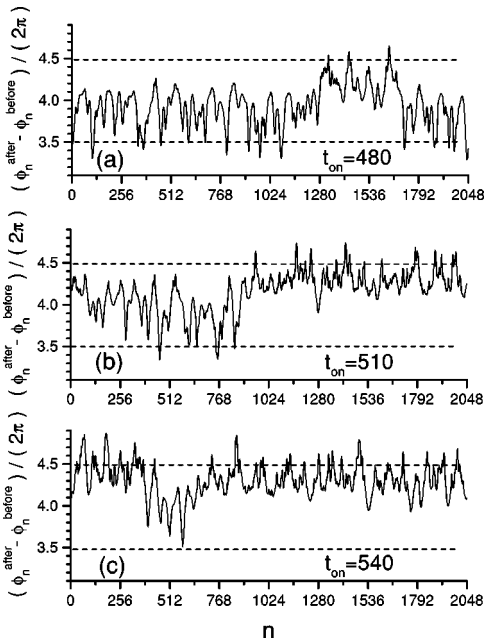

FIG. 15. CDW phase difference from just before the pulse to just after, as a function of position. Numerical data are for steady state, and correspond to the numerical data of Fig. 13. Unlike the strong pinning numerical data, the weak pinning numerical data is not heavily weighted at 3.5π and 4.5π.

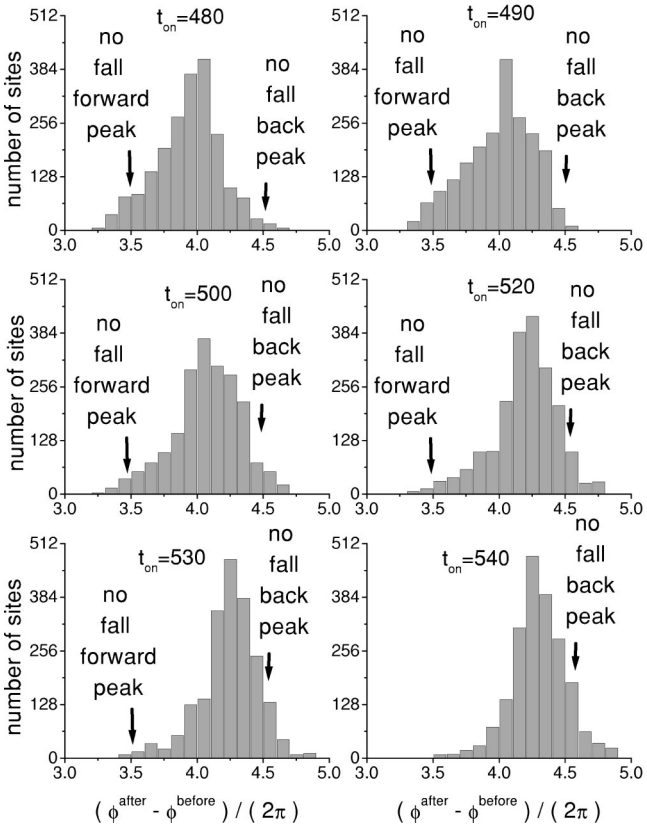

FIG. 16. Histograms of the CDW phase difference from just before the pulse to just after, for six different t_{on} values for the 4/1 step. Numerical data are for steady state, and correspond to the numerical data of Fig. 13. Note that this weak pinning numerical data is not bimodal. The absence of weight near the fall-forward (3.5π) and fall-back (4.5π) regions strongly suggest an absence of phase organization.

In summary, we find that the 1D FLR model exhibits phase organization in the strong pinning limit with highly strained initial conditions. As the pinning strength is decreased the learned behavior gradually degrades. However for no set of model parameters did we observe phase organization starting from initial conditions near the ground state. Also for no set of model parameters could we simulate the experimental observation that the CDW current finishes the pulse at a point of maximum velocity.

V. DISCUSSION

The experiments and numerical simulations reported here find a few features that are qualitatively consistent with the theory of phase organization, but even more that are not. The observations that are consistent with the theory of phase organization are the following.

1. As the number of metastable pinned states accessible to the system decreases ($|I_{low}| \rightarrow I_T$), the PDME degrades.

2. Contrary to previous reports[8] the PDME does not degrade at large drive amplitude ($I_{high} > 3I_T$) in highly coherent samples.

The observations that are inconsistent with the theory of phase organization are the following.

1. There is no beating in the experimental wave forms (Figs. 1–5). This indicates that there is no dephasing and rephasing of the CDW, implying that the internal degrees of freedom of the CDW do not form fall-forward and fall-back regions.

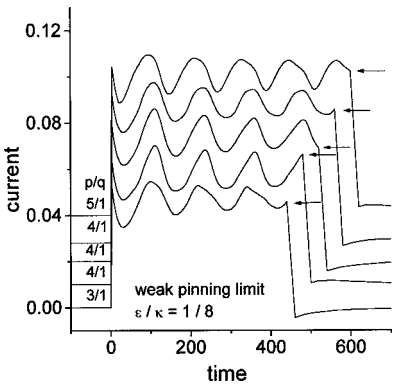

FIG. 17. Numerical simulation data similar to that shown in Fig. 13, the only difference being that the initial conditions are a metastable state near the ground state, and the pulse lengths from bottom to top are 440, 480, 520, 560, and 600. The main point of this figure is that for initial conditions near the ground state, the wave forms are very similar to the single-coordinate model since the current oscillation can finish the pulse increasing or decreasing. We also note that for different initial conditions, the system can mode lock into a different p/q cycle in steady state.

2. Experimentally the CDW current finishes the pulse at a point of maximum velocity, and not at a point of maximum potential energy. Okajima and Ido observe the same behavior for $NbSe_3$,[8] and Abdezzahid and Dumas observe this behavior in high-quality crystals of blue bronze.[9]

3. The spin-density wave (SDW) in $(TMTSF)_2PF_6$ also exhibits the PDME. Contrary to the CDW in $NbSe_3$ the SDW appears to finish the pulse at a point of minimum velocity.[23] After training the voltage response finishes the pulse at a sharp maximum, but there is a noticeable lack of NBN oscillations before the end of the pulse.

4. Numerical simulations observe no learning in the weak pinning limit. As previously discussed, all $NbSe_3$ samples from this study are well into the weak pinning limit.

5. Experimentally the density wave only needs a few training pulses to learn the length of the pulse. Fleming and Schneemeyer find for blue bronze that if the length of the pulse is suddenly increased, it takes only one training pulse for the CDW to learn the length of the new pulse width.[7] For the SDW in $(TMTSF)_2PF_6$, the relearning time is again only one pulse.[23] For $NbSe_3$, we and Okajima and Ido find that it takes only a few training pulses.[8,24] The theory of phase organization predicts that the number of relearning pulses is much greater than one.[11]

6. As discussed in detail by Ito, in the strong pinning limit the FLR model does not exhibit learning for initial conditions near the ground state.[15] Learning only occurs if the strain energy of the initial condition is greater than the strain energy of all the steady-state metastable configurations that are available between pulses. We refer to this as the ground-state paradox.

What we find so intriguing is that experimentally the PDME is robust over a large region of drive parameter space (see Figs. 1–3), yet this learned behavior is apparently not properly described by the FLR model. This type of learned behavior might occur in the FLR model in two or three spa-

tial dimensions. However, according to Ref. 11 phase organization only requires a large number of coupled degrees of freedom, and is independent of spatial dimension. If the FLR model can reproduce the PDME in higher spatial dimension it will be due to a different mechanism.

More likely the essential physics of the PDME is absent from the FLR model. Okajima and Ido,[8] and also Ito[15] have suggested that amplitude collapse cannot be neglected, and that the PDME is due to the organization of slip events. Okajima and Ido previously speculated that phase-slip events near strong pinning centers organize their timing upon application of a repetitive drive sequence, although they provide no numerical evidence for this mechanism.[8]

We speculate that a different type of mechanism is responsible for the PDME. At the contacts normal carriers are converted into CDW carriers. This process involves the formation of dislocations in the CDW superlattice. Mode locking of the CDW to a repetitive pulse sequence requires that these dislocations organize themselves. Upon training, as the CDW polarizes, the strain of the metastable state into which the CDW relaxes between pulses grows until the CDW mode locks. Once mode locking occurs, the superlattice strain no longer grows. During training, we believe the CDW selects a special metastable state such that the amplitude dislocation is expanding most rapidly at the end of the pulse. This leads to a voltage minimum at the end of the pulse, and hence the PDME. This scenario requires further experimental and numerical investigation.

VI. CONCLUSIONS

We have performed a critical comparison between experiment and the theory of phase organization in order to test whether phase organization provides a plausible mechanism of the PDME in $NbSe_3$. We find that it does not. The phase degrees of freedom of the CDW, as described by the FLR model, cannot account for the remarkable learned behavior in these crystals. We agree with Okajima and Ido[8] that amplitude collapse is a key ingredient in the learning mechanism. Theoretical investigations of the organization of dislocations in the CDW superlattice under the application of a repetitive pulse sequence is required. These investigations should open a new direction in the study of learned behavior in nonlinear systems.

ACKNOWLEDGMENTS

We would like to acknowledge many useful discussions with S. E. Brown and S. N. Coppersmith. This work was supported by Clemson University. For a short video clip illustrating the PDME in $NbSe_3$ visit http://physicsnt.clemson.edu/People/mccarten/research.htm.

[1] For a review of sliding charge density-wave transport see, e.g., G. Gruner, Rev. Mod. Phys. **60**, 1129 (1988); P. Monceau, in *Electronic Properties of Quasi-One-Dimensional Materials*, edited by P. Monceau (Reidel, Dordrecht, 1985), Pt. II, p. 139; R. E. Thorne, Phys. Today **49**, 42 (1996), and references therein.

[2] J. C. Gill, Solid State Commun. **39**, 1203 (1981).

[3] J. C. Gill and A. W. Higgs, Solid State Commun. **48**, 709 (1983).

[4] K. Tsursumi, R. Tamegai, S. Kagoshima, and M. Sato, J. Phys. Soc. Jpn. **54**, 3004 (1985).

[5] A. Arbaoui, J. Dumas, E. B. Lopes, and M. Almeida, Solid State Commun. **81**, 567 (1992).

[6] T. L. Adelman, M. C. de Lind van Wijngaarden, S. V. Zaitsev-Zotov, D. DiCarlo, and R. E. Thorne, Phys. Rev. B **53**, 1833 (1996).

[7] R. M. Fleming and L. F. Schneemeyer, Phys. Rev. B **33**, 2930 (1986).

[8] Y. Okajima and M. Ido, Phys. Rev. B **40**, 7553 (1989).

[9] A. Arbaoui, Ph.D. thesis, Centre National de la Recherche Scientifique, Grenoble, 1993.

[10] S. N. Coppersmith, T. C. Jones, L. P. Kadanoff, A. Levine, J. P. McCarten, S. R. Nagel, S. C. Venkataramani, and Xinlei Wu, Phys. Rev. Lett. **78**, 3983 (1997).

[11] C. Tang, K. Weisenfeld, Per Bak, S. N. Coppersmith, and P. Littlewood, Phys. Rev. Lett. **58**, 1161 (1987).

[12] S. N. Coppersmith and P. B. Littlewood, Phys. Rev. B **36**, 311 (1987); S. N. Coppersmith, Phys. Lett. A **125**, 473 (1987); Physica D **51**, 131 (1991).

[13] P. Bak, C. Tang, and Kurt Wiesenfeld, Phys. Rev. Lett. **59**, 381 (1987); *How Nature Works, The Science of Self-Organized Criticality* (Springer-Verlag, New York, 1996).

[14] S. Sinha and W. L. Ditto, Phys. Rev. Lett. **81**, 2156 (1998).

[15] H. Ito, J. Phys. Soc. Jpn. **58**, 1968 (1989); **58**, 1985 (1989).

[16] E. Sweetland, C-Y. Tsai, B. A. Winter, J. D. Brock, and R. E. Thorne, Phys. Rev. Lett. **65**, 3165 (1990).

[17] J. McCarten, D. A. DiCarlo, M. P. Maher, T. L. Adelman, and R. E. Thorne, Phys. Rev. B **46**, 4456 (1992).

[18] J. Levy and M. Sherwin, Phys. Rev. Lett. **67**, 2846 (1991); J. Levy, Ph.D. Thesis, University of Califoria at Santa Barbara, 1993.

[19] D. S. Fisher, Phys. Rev. B **31**, 1396 (1985).

[20] H. Fukuyama, J. Phys. Soc. Jpn. **41**, 513 (1976); H. Fukuyama and P. A. Lee, Phys. Rev. B **17**, 535 (1978); P. A. Lee and T. M. Rice, Phys. Rev. B **19**, 3970 (1979).

[21] H. Matsukawa and H. Takayama, Physica B & C **143**, 80 (1986).

[22] H. Matsukawa and H. Takayama, J. Phys. Soc. Jpn. **56**, 1507 (1987); H. Matsukawa, *ibid.* **56**, 1522 (1987).

[23] T. Yamaguchi, M. Maesato, and S. Kagoshima, J. Phys. Soc. Jpn. **65**, 3438 (1996).

[24] T. C. Jones, Xinlei Wu, C. R. Simpson, Jr., and J. P. McCarten (unpublished).